Nanodiamond-decorated silica spheres as a chromatographic material

*Zuqin Xue, John C. Vinci, and Luis A. Colón**

Department of Chemistry, Natural Sciences Complex, University at Buffalo, The State University of New York, Buffalo, New York 14260-3000, United States

KEYWORDS: detonation nanodiamonds, primary nanoparticles, organosilica, surface modification, hydrogenation, stationary phase, HPLC

ABSTRACT: Nanodiamond (ND) particles (~5 nm), obtained from detonation soot, were oxidized and/or thermally hydrogenated. Both, the non-hydrogenated and hydrogenated ND particles were successfully coupled to the surface of micron-size organo-silica particles. A thin layer of nanodiamonds (NDs) decorating the surface of the organo-silica particles was visible on transmission electron microscopy (TEM) images. X-ray photoelectron spectroscopy (XPS) and infrared spectroscopy (IR) were used to characterize the NDs prior to coupling and to confirm attachment onto the organo-silica particles. Both, ultraviolet (UV) radiation and a chemical initiator were proved to be effective radical initiators for the ND-silica coupling reaction, although for scale up purposes the chemical initiation was more advantageous to produce the ND-silica composite. Commercially available nanodiamond primary particles were also coupled

to the surface of silica particles. The ND-containing silica particles were packed into chromatographic columns to study their initial feasibility as adsorbent material for liquid chromatography. The organo-silica particles decorated with hydrogenated NDs showed to possess reversed phase type (i.e., hydrophobic) behavior towards the probe compounds, while silica particles decorated with the non-hydrogenated NDs showed polar (i.e., hydrophilic) interactions, both under liquid chromatographic conditions.

INTRODUCTION

Nanodiamonds (NDs), diamond particles with size less than ca. 50 nm, have become increasingly available as they can be produced on a large scale by the detonation of carbon-containing explosives (e.g., trinitrotoluene and hexogen) under a non-oxidizing atmosphere;[1-3] hence, the name detonation nanodiamonds (DNDs) is commonly used (herein, DND or ND will be used interchangeably). The DNDs are typically formed as aggregates composed of primary particles (sizes of 4-5 nm)[4-8] with narrow size distributions.[6] One challenge for the use of ND primary particles is their strong tendency toward agglomeration.[9] Covalent bonds and ionic interactions, in addition to van der Waals forces, hold the agglutinates together; graphitic carbon can also be part of these agglutinates.[10,11] Primary particles of DNDs forming these strong aggregates are difficult to be suspended in solution by conventional means.[8] After purification of the detonation soot, extra steps are required to break down the agglomerations into stable colloids of ND primary particles.[9-12] Methods have been developed to isolate primary particles of DNDs in solution, such as by sugar- or salt-assisted milling,[10] laser dispersion,[13] and sonication/milling in the presence of ceramic beads.[8,14] The Ōsawa group has developed the milling method of bead-assisted sonic disintegration (BASD) using small zirconia beads and

ultrasonication to suspend ND primary particles in very polar solvents such as water, dimethyl sulfoxide (DMSO), or methanol to form a stable colloidal solution.[11,14]

As the production cost of NDs has continued to decline,[15] the practicality of various applications has increased and the research on NDs has augmented considerably.[3,16-19] NDs have been exploited to improve mechanical strength of polymers,[20] as a galvanic coating,[18] for biological imaging applications,[21-25] for drug delivery,[12,18,26,27] for precision polishing applications,[3] as lubricants,[18] for magnetic recording,[18] as sensors,[28,29] for catalysis,[30,31] and others.[32,33] Surface functionalization of NDs has become the key for wider applications.[24,34-36] During the post-synthesis treatment and purification, the surface of the ND can be modified to obtain a variety of functional groups that include carboxylic groups, lactones, ketones, hydroxyl groups, halogens, as well as others.[36-39] The surface modification can be realized in the presence of various gaseous media such as H_2, NH_3, F_2, Cl_2, or CCl_4.[12,34,40,41] Various wet chemistry procedures have also been used.[42-44]

The diamond surface has been particularly attractive to researchers in the field of chromatography because of its known adsorptive properties and surface tunability, along with numerous other benefits such as stability with regards to harsh chemical conditions and temperatures.[19,45-47] Nesterenko, et al., have investigated the chromatographic performance of diamond particulates, including 1.2 μm high pressure high temperature (HPHT) synthesized diamond particles.[48] However, the direct use of diamond primary particles, the fundamental building blocks of DND clusters, has yet to be explored as a chromatographic material and stationary phase. The surface of NDs has shown useful adsorptive capabilities,[12,49] as well as surface modifications and ease of derivatization,[19] which can facilitate the possibility of exploring diverse selectivity and interactions for chromatographic applications. Non-spherical and

irregularly shaped sintered ND micro-particulates have been used as stationary phase for liquid chromatography.[50] However, the irregularly shaped particles lead to separation efficiency limitations of the resulting particle-packed chromatographic column.[51] At the same time, it is difficult to obtain uniform micron or submicron sized diamond particulates by detonation due to the nature of the reaction.[12] The duration of the detonation shock wave sets up the size limit because only during that period is there sufficient pressure for the formation of diamond soot.[12] It is obvious that obtaining monodisperse, spherical micron-sized diamond particles suitable for high efficiency HPLC separation is clearly a challenging task.[45]

While DNDs are too small to be packed directly into a column for chromatographic applications; it would be more practical to attach the primary ND particulates (~5 nm) onto a support material, like silica or carbon. Core shell (pellicular, superficially porous) silica particles had emerged as a new generation of packing materials for HPLC. Due to their high efficiency and low backpressure, HPLC columns packed with core shell silica particles with diameter as low as 1.3 μm have been commercialized by major HPLC column manufactures.[52] However, the direct use of nano-sized primary ND particulates as the shell materials has rarely been exploited. Liu et al., employed fluorinated nanodiamond to form a coating on glass surface using wet chemistry instead of commonly used chemical vapor deposition (CVD) method.[53] The Linford group reported on micron-size nanodiamond-containing particles prepared by depositing alternate layers of polyallylamine (PAAm) and DND aggregates (~100 nm) on a spherical glassy carbon core.[51,54] Although, this approach produced stable materials used as support for chromatographic application, mostly after chemical modification to impart chromatographic selectivity, it is important to note that the attachment of primary DND particulates onto a substrate to explore their potential chromatographic interactions has yet to be realized. It is clear

that the application of diamond materials to directly achieve an HPLC separation would ideally use spherical particles with diameter in the low micrometer range having tunable surface functionality. The untapped potential of 4-5 nm DND primary particles as adsorbent materials for chromatographic applications can be exploited by coupling them directly to monodisperse, spherical chromatographic particulates (e.g., silica) to construct a diamond surface. NDs attached to the surface of a solid support material may encounter many potential applications; however, given our interest in chromatographic media, we are interested in studying NDs attached to silica materials as adsorbent for chromatography. Herein, we describe the direct attachment of DND primary particles onto micron-size spherical silica particles. Both, hydrogenated and non-hydrogenated NDs were investigated for such a purpose.

EXPERIMENTAL SECTION

Materials. Tetraethoxylsilane (TEOS) and allyltriethoxylsilane were obtained from Gelest, Inc. (Morrisville, PA). Standard detonation nanodiamond (DND) powder was acquired from the International Technology Center (Raleigh, NC), and NanoAmando primary particle solution of nanodiamonds was acquired from the NanoCarbon Research Institute (Ueda, Japan). Zirconia beads (30 μm diameter), YTZ grinding media, were kindly donated by the Tosoh Corporation (Tokyo, Japan). Benzoyl peroxide (BPO) and toluene were purchased from Sigma-Aldrich (St. Louis, MO). HPLC-grade methanol, HPLC-grade acetonitrile, potassium bromide, and dimethyl sulfoxide (DMSO) were obtained from Fisher Scientific (Fair Lawn, NJ). Ethanol (200 proof) was purchased from Decon Laboratories, Inc. (King of Prussia, PA). Dichloromethane, nitric acid (HNO_3, 65%), and isopropanol were purchased from Mallinckrodt Baker (Phillipsburg, NJ). Sulfuric acid (H_2SO_4, 96.5%) and hydrochloric acid (HCl) were obtained from EMD Millipore (Billerica, MA). Hydrogen gas and ammonia gas (anhydrous),

both of 99.995% purity, were acquired from Praxair (Danbury, CT). A Barnstead International EASYPure II water purification system was used to obtain 18.2 MΩ-cm deionized and filtered (0.2 μm) water, which was used throughout.

Synthesis of Silica Particles. Silica and organo-silica particles were synthesized by the method previously described, with slight modifications, producing non-porous, monodisperse particles.[55,56] For a typical small-scale synthesis of allyl-silica hybrid particles, ethanol (75 mL) and water (45 mL) were added to a graduated 250-mL round bottom flask that contained a stir bar and was sealed with a septum. The flask was lowered into a cooling bath (Neslab endocal RTE-100LP) at a temperature of -10 °C that also contained a small stirring plate. Ammonia gas was pumped into the flask immersed in the low temperature bath. After the total volume in the flask reached 225 mL and the temperature of the solution was at -10 °C, 4 mL of tetraethoxylsilane (TEOS) and 200 μL of allyltriethoxylsilane (allyl-TrEOS) were added to the flask. To obtain bare-silica, only the TEOS was added. The solution was stirred constantly, and after 1 hour the temperature was adjusted to 0 °C. After 1 hour at 0 °C, the temperature was adjusted to 25 °C. The synthesized particles were subjected to repeated washing/centrifuging steps with ethanol, isopropanol, 50 mM aqueous HCl, and water in glass centrifuge tubes using an IEC clinical centrifuge at 998 ± 10 RPM (7.5 cm rotor) and allowed to dry overnight at 120 °C.

Modification and Processing of Nanodiamonds. Prior to use, DND powder was treated with 90% H_2SO_4/10% HNO_3 (by volume) at 140 °C for 4 hours. After cooling the acidic solution of treated powder, multiple centrifuging/washing steps with water were performed until the pH of the washes was measured to be neutral using pH paper. A Costar Mini-centriguge (2.5 cm rotor) at 10, 000 RPM was used. These acid-washed, oxidized DNDs constitute the "O-ND"

sample. For hydrogenation, ~0.06 g of DND powder was exposed to 100 sccm H_2 gas for 5 hours at 900 °C in a Thermo (Waltham, MA) Lindberg/Blue M tube furnace. These hydrogenated DNDs constitute the "H_2-ND" sample. Both O-ND and H_2-ND powders were suspended in DMSO to produce primary particles in solution by the bead-assisted sonic disintegration (BASD) method.[14] Briefly, 7.5 g of the 30 μm zirconia beads were mixed with either 0.050 g of O-ND or H_2-ND powder and placed into 2 mL of DMSO. The resulting suspension was horn sonicated with a 1/8" Ti probe operating at 50% power for 3 hours. The horn sonicator was model Q500 from QSonica (Newtown, CT) with the maximum power rating of 500 watts and a frequency of 20 kHz. The commercially available NanoAmando ND primary particle solution was used as-received without any further processing, and these DNDs without any modifications constitute the commercial "C-ND" sample.

Nanodiamond-Silica Coupling. NDs were attached to allyl-silica via radical coupling. Hydrogen abstraction was achieved via ultraviolet (UV)-light photo-initiation or by chemical-initiation with BPO. UV-light photoinitiation was used to produce ND-silica particles in a small-scale, while chemical initiation was used to prepare particles in a larger scale that were consequently packed into a column for chromatographic testing. For the small-scale coupling, an amount of either ~25 mg of either O-ND or H_2-ND primary particles were used, which were already suspended in DMSO. The total volume of DMSO containing the primary particles was brought up to a total volume of 3 mL and 100 mg of allyl-silica was added, mixed, and bath sonicated to form a slurry solution. The slurry was carefully transferred to an open 4 mL glass vial containing a small stir bar. UV radiation from a mercury pen-lamp light-source (Newport/Oriel, Irvine, CA) was placed directly above the stirred slurry inside the vial. The glass vial was wrapped in aluminum foil and allowed to react under the UV lamp for 24 hours in a

dark room. After reaction, the slurry was immediately centrifuged and washed. The centrifuging/washing steps included 3x repeats each with DMSO, water, and acetone. Then the solid was re-suspended in DMSO for bath sonication for 1 hour. The washing and sonication was repeated twice. A third washing/centrifuging step with the 3x repeats per solvent was performed before the product was dried at 60 °C for 20 hours in a Precision (Thermo Fisher Scientific, Waltham, MA) vacuum oven. These materials constituted the O-ND-allyl-silica and H_2-ND-allyl-silica modified samples. Control reactions under dark were performed for both ND-allyl-silica products. For the dark control reactions, all reaction conditions and post-synthetic workup was performed the same way with the exception of the UV radiation.

The commercially available NanoAmando primary particles, already in solution (i.e., C-NDs), were coupled to silica particles by using benzoyl peroxide (BPO) as the free radical initiator (see Scheme S1 in SI). In a typical reaction, DMSO (12 mL) was mixed with BPO (0.15 g) until dissolved. Then, 400 mg allyl-silica was added and sonicated to form a slurry solution. Next, C-NDs (5% solution, 3 mL) were added and the mixture was sonicated again. Then, the slurry was stirred and maintained at 75 °C for 3 hours using a temperature-controlled microwave oven from Microwave Research & Applications (Carol Stream, IL). This product was washed/centrifuged as described above. For even larger quantities of modified silica particles suitable for packing into an HPLC column, DMSO (24 mL) was mixed with BPO (0.30 g) until dissolution occurred. Then, 800 mg allyl-silica was added and bath sonicated until a well-suspended slurry solution was formed. Next, H_2-NDs (5% solution, 1 mL) or C-NDs (5% solution, 3 mL) were added and bath sonicated again. The slurry was kept at 90 °C for 5 hours with stirring. The product for each was washed/centrifuged as described above, constituting the H_2-NDs-allyl-silica or the C-NDs-allyl-silica samples for HPLC column packing.

Characterization. Transmission electron microscopy (TEM) imaging, including high-resolution TEM (HRTEM), was accomplished with a JEOL (Peabody, MA) JEM 2010 system operated at 200 kV. Selected area electron diffraction patterns were also obtained within the electron microscope setup. Samples for TEM were evaporated on an ultrathin carbon film on copper grids or ultrathin carbon on holey carbon on copper grids acquired from Ted Pella (Redding, CA). Scanning electron microscopy (SEM) imaging was performed on a Hitachi (Tokyo, Japan) SU-70 field emission scanning electron microscope (FESEM) with Oxford energy-dispersive X-ray spectrometer (EDS). Samples for SEM were smeared as dry powder on a PELCO tab purchased from Ted Pella (Redding, CA). The size of the silica and ND-silica hybrid particles was estimated by measuring at least 100 particles from a TEM image using the public domain ImageJ software (National Institutes of Health). Particle size distributions of NDs were obtained with dynamic light scattering (DLS) measurements performed at 25 ˚C on a Malvern (Worcestershire, UK) ZetaSizer with a disposable plastic cuvette. Surface area analysis was achieved with a Micromeritics ASAP2010 gas adsorption analyzer (Norcross, GA). The particles were prepared by drying at 250 °C for up to 6 hours under vacuum using nitrogen as the gas adsorbate. Surface area was determined by the Brunauer-Emmet-Teller (BET) method. X-ray photoelectron spectroscopy (XPS) measurements were performed under high vacuum conditions using a Physical Electronics (Chanhassen, MN) PHI 5000 VersaProbe XPS spectrometer with monochromatic Al Kα radiation (1486.6 eV) equipped with a hemispherical energy analyzer. Samples were drop-cast onto a silicon wafer and analyzed with pass energy of 23.5 eV and 0.1 eV increment for high-resolution scans and pass energy of 117.4 eV and 1.0 eV increment for survey scans. PHI Multipak software (version 9.2.0.5) was used for relative elemental analysis from high-resolution scans of C1s, O1s, and Si2p. Diffuse reflectance infrared Fourier transform

(DRIFT) spectroscopy was performed at room temperature under atmospheric conditions with a PerkinElmer (Waltham, MA) Spectrum Two (2 cm^{-1}, 300 scans). Samples were prepared by mixing 1 mg particles with 19 mg of potassium bromide. The mixture was ground into fine powder using an agate mortar and pestle.

Column Packing for HPLC. To pack HPLC columns, 400 mg of particles (either bare silica, allyl-silica, C-ND-allyl-silica, or H_2-ND-allyl-silica particles) were mixed with 5 mL of methanol and sonicated for 30 min. The suspension was immediately transferred to a 5-mL column-packing reservoir attached to a 3 mm inner diameter x 3 cm length column equipped with a 0.5 μm frit at the outlet end of the column. Column hardware and frits were purchased from Idex (Lake Forest, IL). The columns were packed at 12, 000 psi with methanol as the push solvent using a Haskel (Burbank, CA) high-pressure packing pump. HPLC experiments were carried out with an Agilent 1100 system from Agilent Technologies (Palo Alto, CA) equipped with a diode array detector. Data collection and system operation were through the ChemStation for LC 3D (Rev. A.09.03) software from Agilent Technologies. All the LC experiments were carried out at room temperature around 22 °C. Acetonitrile, water, and mixtures thereof were used as mobile phases. All samples and mobile phases were filtered through 0.45 μm filters, and mobile phases were degassed prior to use.

RESULTS AND DISCUSSION

Nanodiamonds. NDs displayed extensive aggregation when not in solution, as seen by TEM imaging in Figure 1A for O-ND nanoparticles deposited from solution. The distinct diffraction ring-patterns, however, confirmed the existence of the diamond structure (Figure 1B). NDs also exist as large aggregates in solution; they were effectively de-aggregated into primary particles by a bead-assisted sonic disintegration (BASD) method.[14,57] There was a clear visible

change in appearance before and after BASD, from a gray slurry solution before BASD to a dark brown solution after the sonication procedure (Figure 1C-D). Particle size distribution of the agglutinates and primary particles were monitored by dynamic light scattering (DLS) measurements (e.g., Figure 1E). The agglutinates in Figure 1E showed an average size around 255 nm in solution before sonication while the great majority of particles exhibited a size of about 6 nm after sonication for three hours; a very small fraction of NDs showed a size centered at 24 nm. Considering the hydrodynamic radius in solution, the observed 6 nm size is consistent with the size of primary particles.[14,36,57] The NDs particles obtained after applying the BASD method to both oxidized and hydrogenated NDs were used to react with silica spheres to synthesize the ND-silica composites (*vide infra*).

In our initial approach to produce silica particles containing NDs at the surface, we explored the use of hydrogenated and non-hydrogenated NDs. Thermal hydrogenation of ND under hydrogen gas flow at elevated temperatures has provided a convenient route for surface chemical modification.[40,58,59] We first started with detonation powder (i.e., soot), which was processed as described in the experimental section. Figure 2 depicts DRIFT spectra of hydrogenated NDs (H_2-NDs) and non-hydrogenated NDs (O-NDs). The spectrum of O-NDs showed several bands attributed to O–H stretching (3200-3600 cm^{-1}) that can be related to adsorbed water and possibly to hydroxyl groups on the NDs related to carboxylic acids and alcohols.[60] Other functional groups typically found on oxidized NDs can also be identified, for example, C–O–C (1000-1370 cm^{-1} typical of ethers, acid anhydrides, lactones, epoxy groups), O–H stretching at 2495 cm^{-1} from carboxylic groups, C=O peak at 1750 cm^{-1}, and C– O (589 cm^{-1} and 855 cm^{-1}).[40,60-62] The abundance of bands corresponding to oxygen containing species (OH, C=O and C–O) is indicative of a heavily oxidized ND surface as a result of the acid treatment.

Nevertheless, the spectrum shows that the oxidized NDs also contained sp^3 C–H stretching vibrations in the 2800-3000 cm^{-1} region, which is also characteristic of diamond.[40,61] After thermal hydrogenation, a significant increase in intensity and well-defined peaks in the region of the sp^3 C–H stretching vibrations (particularly the symmetric stretching at 2878 cm^{-1} and asymmetric stretching at 2943 cm^{-1}) were observed.[59] The appearance of C–H peaks at 795 cm^{-1}, 918 cm^{-1} and 1664 cm^{-1} as well as a peak for C–C at 1571 cm^{-1} are also apparent. At the same time, the intensities of peaks assigned to oxygen-containing groups were largely reduced. This significant change of the spectrum is indicative of the ND surface hydrogenation. Although herein we explored the extremes (i.e., NDs with a high degree of oxidation and a high degree of hydrogenation), it is important to note that by adjusting temperature and/or reaction time one can control the degree of hydrogenation,[40,58,59] which in turn can provide NDs with different surface polarity with potential impact on selectivity for chromatographic applications.

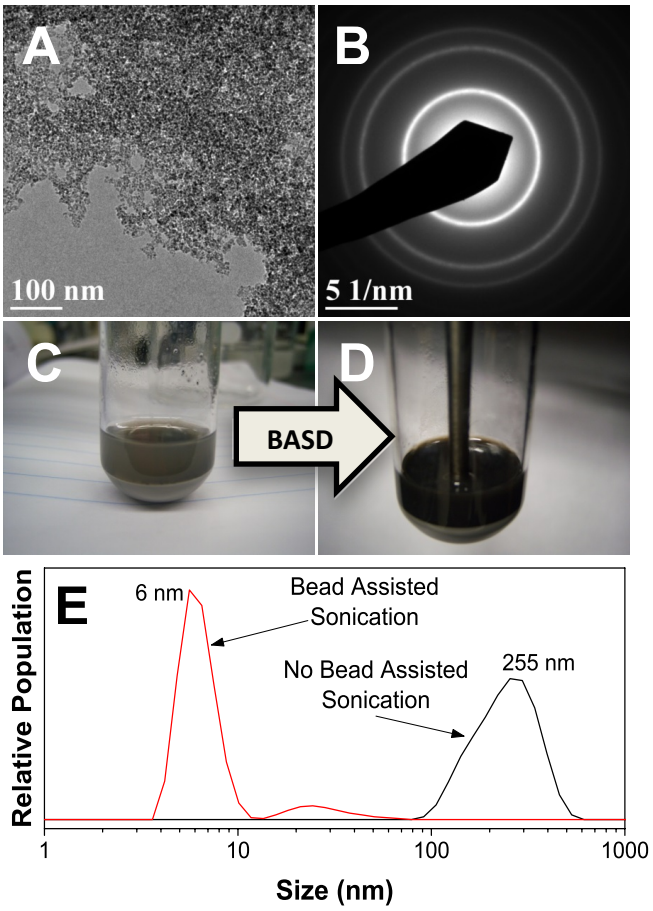

Figure 1. A) TEM image of ND powder aggregates, B) selected area electron diffraction pattern of the ND powder aggregates. The electron diffraction ring patterns correspond to the crystal structure of diamond, and the intense center ring corresponds to the (1 0 3) diffraction plane of diamond. C) Image of the greyish ND aggregates in solution before the bead-assisted sonic disintegration (BASD) method. (D) Image of a solution containing primary particles isolated after BASD – the greyish-looking powder on the bottom is the larger zirconia beads that have settled out of solution. E) Particle size distribution of nanodiamonds before and after the BASD.

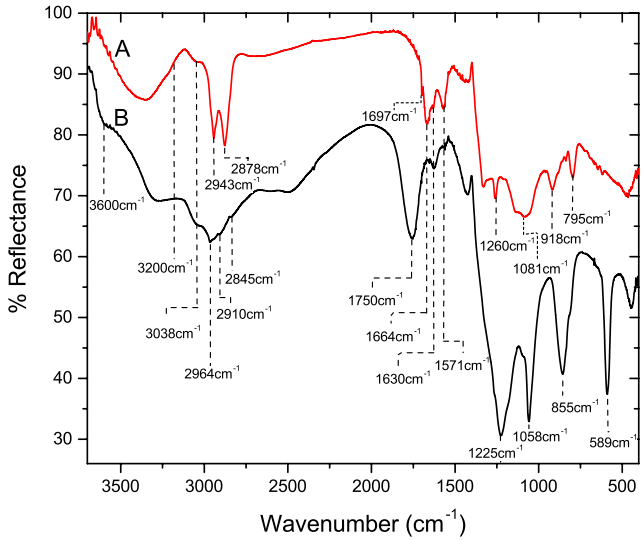

Figure 2. DRIFT spectra of (A) H_2-NDs and (B) O-NDs. For peak assignment to a respective functional group see Tables S1 and S2.

ND-Silica Coupling. To attach NDs to the silica particle surface via reaction with a terminal double bond functionality, one must have such a moiety on the silica surface. This can be achieved by performing a silanization reaction of bare silica particles to introduce the reactive functionality (e.g., allyl or vinyl groups). Our group has synthesized organo-silica hybrid materials containing organic pendants that are more hydrolytically stable than those produced by silanization of bare silica.[55,56,63,64] Herein, we used our procedure to prepare organo-silica hybrid particles containing an allyl pendant on the surface to allow attachment of the NDs to the silica via the terminal double bond functionality. This approach also simplified the silica modification (no need for silanization). SEM images of the synthesized organo-silica displayed spherical particles with a relatively narrow size-distribution approaching 1-μm diameter, similar to bare silica particles synthesized by the same procedure (Figure S1A-B). Using a small mercury lamp to photoinitiate the reaction, H_2-NDs were reacted with the allyl-silica particles. The 254 nm UV

line from a mercury lamp has been shown to be an effective light source for the coupling of terminal double bonds to hydrogenated ND.[58,65-67] The attachment of H_2-NDs on the silica surface was visible under high magnification TEM imaging, as shown in Figure 3. The electron diffraction pattern on a single ND-modified allyl-silica particle (Figure 3C) shows diffraction ring corresponding to the (1 0 3) diffraction plane of diamond.

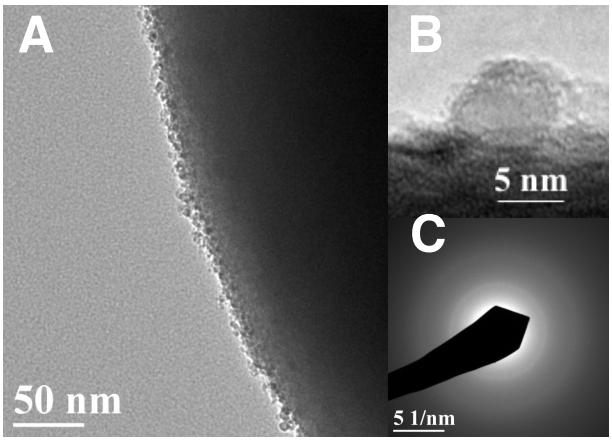

Figure 3. TEM images of A) H_2-ND-modified allyl-silica via UV radiation, b) image of what appears to be a single H_2-ND particle on silica, and C) electron diffraction pattern on a single H_2-ND-modified allyl-silica particle (diffraction ring corresponding to the (1 0 3) diffraction plane of diamond are apparent).

Figure 4 shows the DRIFT spectra of H_2-ND-allyl-silica, allyl-silica, and bare silica. DRIFT spectroscopy confirmed the incorporation of the allyl functionality when compared to bare silica particles. A band at around the 3080 cm^{-1} region of the spectrum can be assigned to the carbon hydrogen stretching of =C–H, while the band around 1635 cm^{-1} can be assigned to the C=C stretch of the allyl group, although superimposed on a band assigned to adsorbed water at

1630 cm^{-1}. The C–H stretch (2978 cm^{-1}) is also apparent on the allyl-silica particle, attributed to the additional hydrocarbon added by introducing the allyl group. Furthermore, XPS experiments showed a drastic increase of carbon content (from 4% to 22%) on the allyl-silica compared to bare silica particles (see Table S3). The observed decrease of the oxygen content in the allyl-silica when compared with bare silica was another indication of the incorporation of allyl groups. The allyl-silica reacted with the H_2-NDs showed a marked decrease of the 1635 cm^{-1} and 3081 cm^{-1} attributed to the allyl groups. The peaks at 1466 cm^{-1} and 1421 cm^{-1} also present on the allyl-silica were greatly reduced. It can also be noted that a band around 1690 cm^{-1} is noticeable in the H_2-NDs allyl-silica, which can be attributed to the C=O functional group present in the NDs, although we cannot discard the possibility of some BPO attachment also. The XPS experiments (Table S1) also showed an increase in the carbon content from 22% on the allyl-silica to 49% on the H_2-NDs allyl-silica, further indicating an incorporation of carbon onto the silica particles. The bare-silica particles displayed a BET surface area of 1 m^2/g, while the allyl-silica had a BET surface area of 11.7 ± 0.1 m^2/g. The BET surface area of the H_2-ND-allyl silica was 13.1 ± 0.1 m^2/g. These last two are similar to each other (~12% increase), which is reasonable given the small layer (~10 nm) of NDs attached at the surface. Overall, however, the experimental evidence indicates that primary particles of H_2-ND have been attached onto the silica surface.

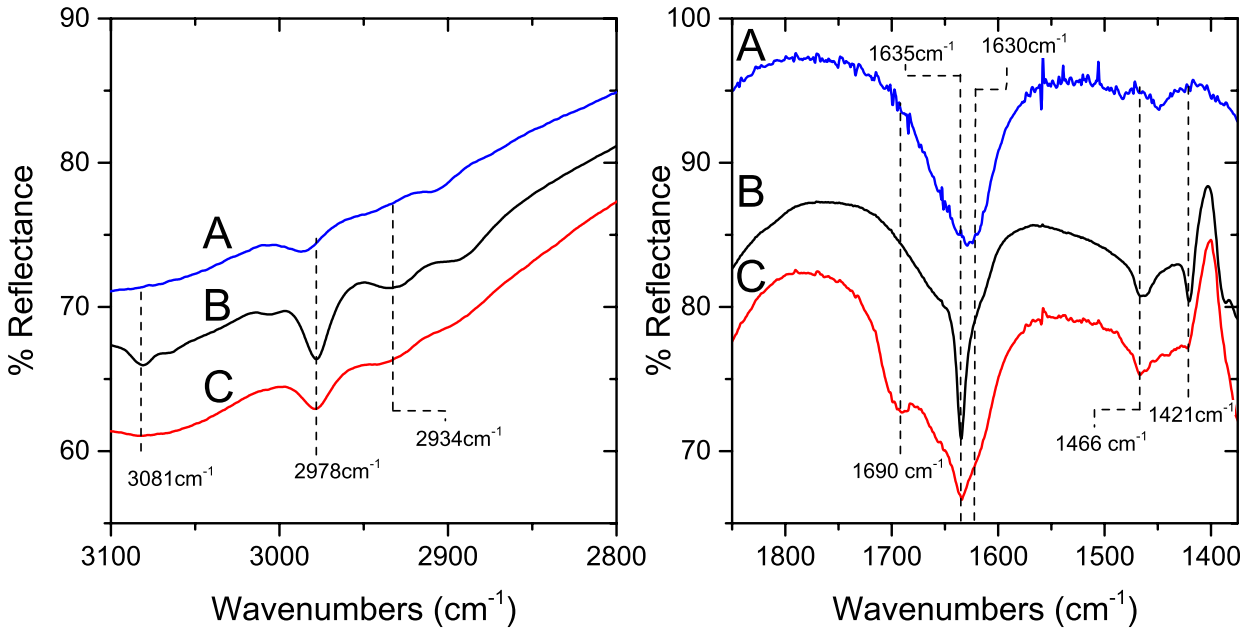

Figure 4. DRIFT spectra of two IR regions for A) bare silica particles, B) allyl-silica particles, and C) H_2-ND-allyl-silica particles. For peak assignment to a respective functional group see Table S4.

The FTIR spectra in Figure 2 showed that both O-ND and H_2-ND contain sp^3 C-H functionality, which can react with the allyl moiety. We reacted O-ND with allyl-silica particles using the same reaction conditions as with the H_2-NDs. TEM imaging of the allyl-silica particles reacted with O-NDs also showed a layer of NDs on the allyl-silica particle surface (Figure 5A). The diffraction pattern (Figure 5C) corresponding to the (1 0 3) diffraction plane of diamond was clearly observed for O-NDs on the allyl-silica. Minimal amounts of O-ND or H_2-ND were adsorbed to the allyl-silica particles in the absence of UV light (Figure S2). The extensive washing, sonication, and rinsing procedures eliminated adsorbed ND material onto the surface of silica. XPS analyses of the ND-decorated silica particles showed the elemental composition of these silica surfaces (see Table S3). The much higher carbon content (49%) is evident on the

silicas reacted with NDs under UV radiation. There was minimal increase for carbon content on the allyl-silica particles mixed with NDs that were not exposed to UV radiation. Overall, allyl groups were responsible for the covalently attachment of NDs under UV radiation.

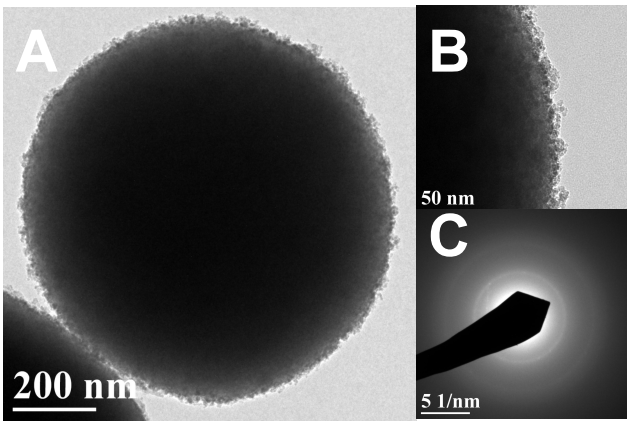

Figure 5. TEM images of A) O-ND-modified allyl-silica via UV radiation, B) larger magnification of a portion of A, and C) electron diffraction pattern on a single O-ND-modified allyl-silica particle (diffraction ring corresponding to the (1 0 3) diffraction plane of diamond are apparent.

The 254 nm UV light source was a convenient way to couple NDs to allyl-silica particles in small proportions. This approach, however, did not prove to be very effective when scaling up the reaction, as the UV light did not penetrate deep into the reaction solution. To scale up the quantity of the ND-silica material suitable for column packing and testing under HPLC conditions we used benzoyl peroxide (BPO) as the radical initiator. BPO has been used for the chemical modification of diamond surface.[68,69] H_2-ND were then reacted with allyl-silica in the presence of BPO. TEM images of the H_2-ND-modified allyl-silica particles showed a layer of NDs on the surface of the silica particles (Figure S3). At this time, we also used commercially

available NDs (C-ND). The DRIFT spectrum of the C-NDs showed peaks corresponding to functionalities that were also observed in both the H_2-NDs and the O-NDs, displaying bands corresponding to stretching vibrations from –OH, C–H, and the oxidative groups (see Figure S4A). However, the intensities corresponding to the sp^3 C–H were more pronounced than those on the in-house produced O-NDs; this makes them particularly desirable for coupling with the allyl-silica. The size distribution from DLS data (see Figure S4B) of C-NDs was comparable to that of the in-house, BASD produced NDs. For the BPO-initiated reaction of the C-NDs and allyl-silica, we first used a temperature-controlled (80 °C) microwave to heat the mixture. TEM images of the C-ND-allyl silica particles showed various clusters of C-NDs on the surface of the ally-silica, most likely due to spotted multiple NDs layers formed by aggregation under the reaction conditions (Figure S5A). We also carried out the reaction under horn sonication to promote de-aggregation of the C-NDs, programmed to also maintain the reaction at a temperature of 80 °C. TEM images (Figure S5B-C) after sonication showed a more uniform layer of C-NDs attached to the allyl-silica surface. Heating at 90 °C in an oil bath also appeared to produce a less spotted and more uniform NDs layer on the allyl-silica (Figure S5D). Figure S5 also suggests that one could control the thickness of the ND layer by manipulating the processing parameters. Increasing the thickness of the ND layer on the particle surface can increase the surface area. Allyl-silica particles having a layer of about 35 nm, for example, showed a surface area of 110.6 ± 0.9 m^2/g.

ND-Silica and HPLC. ND surfaces have shown to possess useful adsorptive capabilities,[12,49] which, along with known surface modifications and ease of derivatization,[19] facilitates their exploration as chromatographic materials. The ND-silica particles composite can provide the beneficial adsorptive properties of the diamond surface without the difficult barrier

of producing high-quality, single-digit micron diamond particles suitable for high-efficiency HPLC separations. To investigate the potential use of the ND-allyl-silica particles as adsorbent materials for liquid chromatography, we packed C-ND-allyl-silica particles into stainless steel HPLC columns; allyl-silica particles (i.e., without NDs) were also packed for comparison. The particles were slurried in methanol and packed at 12,000 psi using MeOH as the push solvent. The packed columns were tested under HPLC conditions; the operating pressure did not exceed 3,000 psi and the columns were stable throughout all testing for both, the C-ND-allyl-silica and the control (allyl-silca particles without NDs). Figure 6 shows a chromatogram displaying the separation of benzene, acetyl salicylic acid, and salicylic acid using bare silica, allyl silica, and C-ND-allyl silica under identical mobile phase conditions. It is clear that the three probes compounds are fully separated in the ND-containing silica. The high content of acetonitrile in the mobile phase favored polar interactions with the stationary phase, reflected by the elution order of the probe compounds (most retained compound was the most polar one). This indicates that the polar groups at the surface of the C-ND-allyl-silica interacted with the probe solutes according to polarity. The observed separation behavior indicates the utility of the column containing the C-ND-allyl-silica for hydrophilic interaction liquid chromatography (HILIC).

The silica composites containing the in-housed hydrogenated-ND were also packed into columns and tested under liquid chromatographic conditions. The hydrogenated NDs rendered a hydrophobic surface on the silica particles, which can act as a reversed phase stationary phase in liquid chromatography. This is observed in the chromatograms shown in Figure 7, where the separation of probe compounds follows the expected reversed phase behavior. Comparison with a column packed with only the ally-silica shows that the separation is possible on the column containing the H_2-ND-allyl-decorated silica but not on the ally-silica column even when the

mobile phase conditions are more favorable for reversed phase interactions in the allyl-silica column.

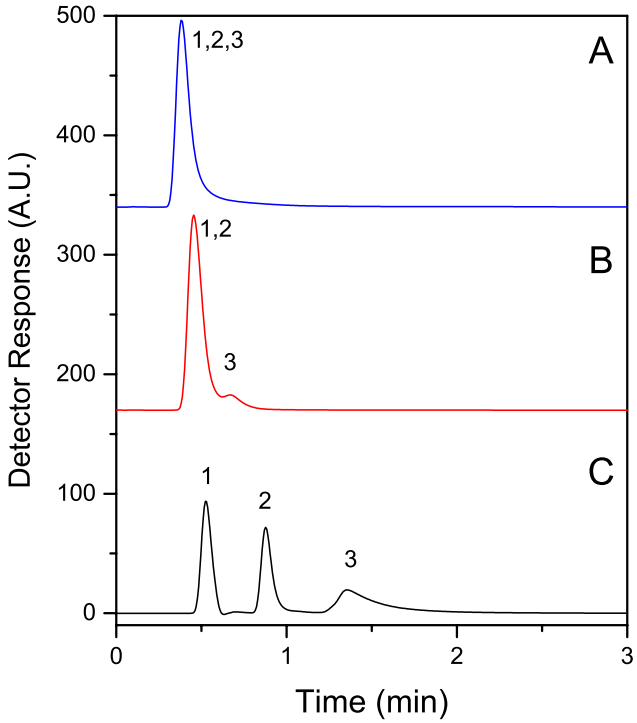

Figure 6. Chromatograms for the separation of three model compounds on columns packed with three different silica particles: A) silica, B) allyl-silica, and C) C-NDs-allyl-silica particles. Column dimensions: 30 mm length x 3 mm i.d., mobile phase: 80% acetonitrile - 20% 20 mM ammonium acetate (pH=7.7), flow rate: 0.25 mL/min, UV detection: 254 nm, injection volume: 5 µL, peaks in order of elution: (1) benzene (1 mM), (2) acetyl salicylic acid (1 mM), (3) salicylic acid (1 mM). Room temperature: ~22 °C.

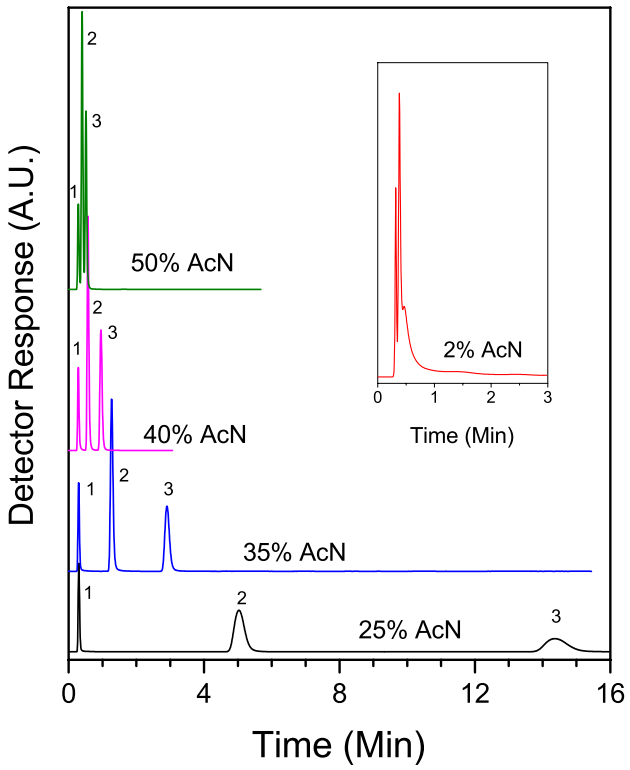

Figure 7. Chromatograms for the separation of three model compounds on a column packed with the H_2-NDs-silica particles at different acetonitrile (AcN)–water mobile phase composition (as indicated). Column dimensions: 30 mm length x 3 mm i.d., flow rate: 0.4 mL/min, UV detection: 254 nm, injection volume: 1 µL, peaks in order of elution: (1) uracil (1 mM), (2) benzophenone (1 mM), (3) biphenyl (1 mM). Room temperature: 20-24 °C. Insert: chromatogram for separation of three model compounds on a column packed with allyl-silica particles with the same chromatographic conditions for the H_2-NDs-silica column.

CONCLUSIONS

We developed a method of attaching NDs to silica particles. Hydrogenated and non-hydrogenated NDs, both containing sp^3 C–H functionality, were coupled via radical initiation to

allyl-containing silica particles. This rendered a solid silica support decorated with a relatively thin layer of NDs. Both, UV light and BPO proved to be effective initiators to couple the NDs to the allyl-silica support. The ND-allyl-silica coupling was confirmed by FTIR, XPS, and TEM spectroscopies, with control experiments showing negligible amounts, if any, present due to adsorption. To prepare relatively larger quantities of the ND-silica composite, BPO was more effective as a radical initiator than UV light. This allowed the preparation of sufficient material to pack columns for an initial assessment of the ND-silica composite as chromatographic media for liquid chromatography.

In the preliminary chromatographic evaluation, we did not attempt to optimize column packing to maximize column efficiency, an aspect that will be considered in the future. It is clear, however, that the ND-decorated particles do provide separation of the test compounds, demonstrating a selective behavior when compared with the material that did not have the NDs. In addition, the ND-silica particles showed separation selectivity depending on the ND surface chemistry. Hydrogenated ND-silica favored hydrophobic interactions while the silica decorated with the commercial NDs, containing more polar groups, showed hydrophilic interactions with the test probes used. Although a thorough chromatographic evaluation is underway after these preliminary results, the ND-silica composites showed promise for both reversed-phase and hydrophilic interaction liquid chromatography, depending on the ND surface. The ND-shell on the silica support can increase material stability over plain silica particles. One can also envision ND surface modifications to tailor the ND-silica material with specific chromatographic selectivity (e.g., C8, phenyl, etc.) Strong, hydrolytic stable linkage on ND can be achieved via Diels-Alder or diazonium coupling procedures.[36,70,71] Herein, we presented the potential application of the ND-decorated silica composite to liquid chromatography; however, we think

that other possibilities exist, where a solid silica support decorated with a diamond surface may be of benefit.

ASSOCIATED CONTENT

Supporting Information. Additional information cited in the manuscript is provided and contains a simplified reaction scheme, SEM and TEM images of silica particles (nanodiamond-modified and unmodified) under different conditions, DRIFT spectrum of C-NDs, and graph showing particle size via dynamic light scattering. In addition, there are tables containing the IR peaks assignments for the DRIFT spectra and XPS data related to the NDs and ND-modified silica particles. This material is available free of charge via the internet at http://pubs.acs.org.

AUTHOR INFORMATION

Corresponding Author

*Phone: 716-645-4213. Fax: 716-645-6963. E-mail: lacolon@buffalo.edu.

Author Contributions

The manuscript was written through contributions of all authors. All authors have given approval to the final version of the manuscript.

ACKNOWLEDGMENT

We acknowledge the financial support for this work by the USA National Science Foundation (CHE 1058373 and CHE 1508105). Any opinions, findings, and conclusions or recommendations expressed in this material are those of the authors and do not necessarily reflect the views of the National Science Foundation.

ABBREVIATIONS

BASD, bead-assisted sonic disintegration; BET, Brunauer-Emmet-Teller; CVD, chemical vapor deposition; C-ND, commercial nanodiamond primary particle solution; DND, detonation nanodiamond; DRIFT, diffuse reflectance infrared Fourier transform; HPHT, high pressure high temperature; HPLC, high performance liquid chromatography; H_2-ND, hydrogenated nanodiamond; ND, nanodiamond; O-ND, oxidized nanodiamond; SEM, scanning electron microscopy; TEM, transmission electron microscopy; XPS, X-ray photoelectron spectroscopy.

REFERENCES

(1) Daulton, T. L.; Eisenhour, D. D.; Bernatowicz, T. J.; Lewis, R. S.; Buseck, P. R., Genesis of Presolar Diamonds: Comparative High-Resolution Transmission Electron Microscopy Study of Meteoritic and Terrestrial Nano-Diamonds. *Geochim. Cosmochim. Acta* **1996,** *60,* 4853-4872.

(2) Krueger, A., Nanodiamond. In *Carbon Materials and Nanotechnology*, Wiley-VCH Verlag GmbH & Co. KGaA: 2010; pp 329-388.

(3) Dolmatov, V. Y., Detonation Synthesis Ultradispersed Diamonds: Properties and Applications. *Russ. Chem. Rev.* **2001,** *70,* 607-626.

(4) Greiner, N. R.; Phillips, D. S.; Johnson, J. D.; Volk, F., Diamonds in Detonation Soot. *Nature* **1988,** *333,* 440-442.

(5) Badziag, P.; Verwoerd, W. S.; Ellis, W. P.; Greiner, N. R., Nanometre-Sized Diamonds Are More Stable Than Graphite. *Nature* **1990,** *343,* 244-245.

(6) Raty, J.-Y.; Galli, G., Ultradispersity of Diamond at the Nanoscale. *Nat. Mater.* **2003,** *2,* 792-795.

(7) Wang, C.; Chen, J.; Yang, G.; Xu, N., Thermodynamic Stability and Ultrasmall-Size Effect of Nanodiamonds13. *Angew. Chem. Int. Ed.* **2005,** *44,* 7414-7418.

(8) Kruger, A.; Kataoka, F.; Ozawa, M.; Fujino, T.; Suzuki, Y.; Aleksenskii, A.; Vul, A.; Osawa, E., Unusually Tight Aggregation in Detonation Nanodiamond: Identification and Disintegration. *Carbon* **2005,** *43,* 1722-1730.

(9) Krueger, A.; Boedeker, T., Deagglomeration and Functionalisation of Detonation Nanodiamond with Long Alkyl Chains. *Diamond Relat. Mater.* **2008,** *17,* 1367-1370.

(10) Pentecost, A.; Gour, S.; Mochalin, V.; Knoke, I.; Gogotsi, Y., Deaggregation of Nanodiamond Powders Using Salt- and Sugar-Assisted Milling. *ACS Appl. Mater. Interfaces* **2010,** *2,* 3289-3294.

(11) Krueger, A.; Ozawa, M.; Jarre, G.; Liang, Y.; Stegk, J.; Lu, L., Deagglomeration and Functionalisation of Detonation Diamond. *Phys. Status Solidi A* **2007,** *204,* 2881-2887.

(12) Krueger, A., The Structure and Reactivity of Nanoscale Diamond. *J. Mater. Chem.* **2008,** *18,* 1485-1492.

(13) Niu, K.-Y.; Zheng, H.-M.; Li, Z.-Q.; Yang, J.; Sun, J.; Du, X.-W., Laser Dispersion of Detonation Nanodiamonds. *Angew. Chem. Int. Ed.* **2011,** *50,* 4099-4102.

(14) Ozawa, M.; Inaguma, M.; Takahashi, M.; Kataoka, F.; Krüger, A.; Ōsawa, E., Preparation and Behavior of Brownish, Clear Nanodiamond Colloids. *Adv. Mater.* **2007,** *19,* 1201-1206.

(15) Schrand, A. M.; Hens, S. A. C.; Shenderova, O. A., Nanodiamond Particles: Properties and Perspectives for Bioapplications. *Crit. Rev. Solid State Mater. Sci.* **2009,** *34,* 18-74.

(16) Ōsawa, E., Recent Progress and Perspectives in Single-Digit Nanodiamond. *Diamond Relat. Mater.* **2007,** *16,* 2018-2022.

(17) Krueger, A., Diamond Nanoparticles: Jewels for Chemistry and Physics. *Adv. Mater.* **2008,** *20,* 2445-2449.

(18) Shenderova, O. A.; Zhirnov, V. V.; Brenner, D. W., Carbon Nanostructures. *Crit. Rev. Solid State Mater. Sci.* **2002,** *27,* 227-356.

(19) Krueger, A., New Carbon Materials: Biological Applications of Functionalized Nanodiamond Materials. *Chem. Eur. J.* **2008,** *14,* 1382-1390.

(20) Li, L.; Davidson, J. L.; Lukehart, C. M., Surface Functionalization of Nanodiamond Particles Via Atom Transfer Radical Polymerization. *Carbon* **2006,** *44,* 2308-2315.

(21) Cheng, C. Y.; Perevedentseva, E.; Tu, J. S.; Chung, P. H.; Cheng, C. L.; Liu, K. K.; Chao, J. I.; Chen, P. H.; Chang, C. C., Direct and in Vitro Observation of Growth Hormone Receptor Molecules in A549 Human Lung Epithelial Cells by Nanodiamond Labeling. *Appl. Phys. Lett.* **2007,** *90,* 163903.

(22) Yu, S.-J.; Kang, M.-W.; Chang, H.-C.; Chen, K.-M.; Yu, Y.-C., Bright Fluorescent Nanodiamonds: No Photobleaching and Low Cytotoxicity. *J. Am. Chem. Soc.* **2005,** *127,* 17604-17605.

(23) Boudou, J.-P.; Curmi, P. A.; Jelezko, F.; Wrachtrup, J.; Aubert, P.; Sennour, M.; Balasubramanian, G.; Reuter, R.; Thorel, A.; Gaffet, E., High Yield Fabrication of Fluorescent Nanodiamonds. *Nanotechnology* **2009,** *20,* 235602.

(24) Krüger, A.; Liang, Y.; Jarre, G.; Stegk, J., Surface Functionalisation of Detonation Diamond Suitable for Biological Applications. *J. Mater. Chem.* **2006,** *16,* 2322-2328.

(25) Fu, C. C.; Lee, H. Y.; Chen, K.; Lim, T. S.; Wu, H. Y.; Lin, P. K.; Wei, P. K.; Tsao, P. H.; Chang, H. C.; Fann, W., Characterization and Application of Single Fluorescent Nanodiamonds as Cellular Biomarkers. *Proc. Natl. Acad. Sci. U. S. A.* **2007,** *104,* 727-732.

(26) Guan, B.; Zou, F.; Zhi, J., Nanodiamond as the Ph-Responsive Vehicle for an Anticancer Drug. *Small* **2010,** *6,* 1514-1519.

(27) Alhaddad, A.; Adam, M. P.; Botsoa, J.; Dantelle, G.; Perruchas, S.; Gacoin, T.; Mansuy, C.; Lavielle, S.; Malvy, C.; Treussart, F.; Bertrand, J. R., Nanodiamond as a Vector for Sirna Delivery to Ewing Sarcoma Cells. *Small* **2011,** *7,* 3087-3095.

(28) Petráková, V.; Taylor, A.; Kratochvílová, I.; Fendrych, F.; Vacík, J.; Kučka, J.; Štursa, J.; Cígler, P.; Ledvina, M.; Fišerová, A.; Kneppo, P.; Nesládek, M., Luminescence of Nanodiamond Driven by Atomic Functionalization: Towards Novel Detection Principles. *Adv. Funct. Mater.* **2012,** *22,* 812-819.

(29) Vlasov, II; Shenderova, O.; Turner, S.; Lebedev, O. I.; Basov, A. A.; Sildos, I.; Rahn, M.; Shiryaev, A. A.; Van Tendeloo, G., Nitrogen and Luminescent Nitrogen-Vacancy Defects in Detonation Nanodiamond. *Small* **2010,** *6,* 687-694.

(30) Jang, D. M.; Myung, Y.; Im, H. S.; Seo, Y. S.; Cho, Y. J.; Lee, C. W.; Park, J.; Jee, A. Y.; Lee, M., Nanodiamonds as Photocatalysts for Reduction of Water and Graphene Oxide. *Chem. Commun.* **2012,** *48,* 696-698.

(31) Pastrana-Martínez, L. M.; Morales-Torres, S.; Carabineiro, S. A. C.; Buijnsters, J. G.; Faria, J. L.; Figueiredo, J. L.; Silva, A. M. T., Nanodiamond-Tio2composites for Heterogeneous Photocatalysis. *ChemPlusChem* **2013,** *78,* 801-807.

(32) Krueger, A., Beyond the Shine: Recent Progress in Applications of Nanodiamond. *J. Mater. Chem.* **2011,** *21,* 12571.

(33) Shugalei, I. V.; Voznyakovskii, A. P.; Garabadzhiu, A. V.; Tselinskii, I. V.; Sudarikov, A. M.; Ilyushin, M. A., Biological Activity of Detonation Nanodiamond and Prospects in Its Medical and Biological Applications. *Russ. J. Gen. Chem.* **2013,** *83,* 851-883.

(34) Spitsyn, B. V.; Davidson, J. L.; Gradoboev, M. N.; Galushko, T. B.; Serebryakova, N. V.; Karpukhina, T. A.; Kulakova, I. I.; Melnik, N. N., Inroad to Modification of Detonation Nanodiamond. *Diamond Relat. Mater.* **2006,** *15,* 296-299.

(35) Chang, I. P.; Hwang, K. C.; Ho, J. A.; Lin, C. C.; Hwu, R. J.; Horng, J. C., Facile Surface Functionalization of Nanodiamonds. *Langmuir* **2010,** *26,* 3685-3689.

(36) Meinhardt, T.; Lang, D.; Dill, H.; Krueger, A., Pushing the Functionality of Diamond Nanoparticles to New Horizons: Orthogonally Functionalized Nanodiamond Using Click Chemistry. *Adv. Funct. Mater.* **2011,** *21,* 494-500.

(37) Jiang, T.; Xu, K., Ftir Study of Ultradispersed Diamond Powder Synthesized by Explosive Detonation. *Carbon* **1995,** *33,* 1663-1671.

(38) Betz, P.; Krueger, A., Surface Modification of Nanodiamond under Bingel–Hirsch Conditions. *ChemPhysChem* **2012,** *13,* 2578-2584.

(39) Krueger, A.; Lang, D., Functionality Is Key: Recent Progress in the Surface Modification of Nanodiamond. *Adv. Funct. Mater.* **2012,** *22,* 890-906.

(40) Ando, T.; Inoue, S.; Ishii, M.; Kamo, M.; Sato, Y.; Yamada, O.; Nakano, T., Fourier-Transform Infrared Photoacoustic Studies of Hydrogenated Diamond Surfaces. *J. Chem. Soc., Faraday Trans.* **1993,** *89,* 749.

(41) Liu, Y.; Gu, Z.; Margrave, J. L.; Khabashesku, V. N., Functionalization of Nanoscale Diamond Powder: Fluoro-, Alkyl-, Amino-, and Amino Acid-Nanodiamond Derivatives. *Chem. Mater.* **2004,** *16,* 3924-3930.

(42) Khanal, M.; Turcheniuk, V.; Barras, A.; Rosay, E.; Bande, O.; Siriwardena, A.; Zaitsev, V.; Pan, G.-H.; Boukherroub, R.; Szunerits, S., Toward Multifunctional "Clickable" Diamond Nanoparticles. *Langmuir* **2015,** *31,* 3926-3933.

(43) Yeap, W. S.; Liu, X.; Bevk, D.; Pasquarelli, A.; Lutsen, L.; Fahlman, M.; Maes, W.; Haenen, K., Functionalization of Boron-Doped Nanocrystalline Diamond with N3 Dye Molecules. *ACS Appl. Mater. Interfaces* **2014,** *6,* 10322-10329.

(44) Wang, Z.; Xu, C.; Liu, C., Surface Modification and Intrinsic Green Fluorescence Emission of a Detonation Nanodiamond. *J. Mater. Chem. C* **2013,** *1,* 6630-6636.

(45) Nesterenko, P. N.; Fedyanina, O. N.; Volgin, Y. V., Microdispersed Sintered Nanodiamonds as a New Stationary Phase for High-Performance Liquid Chromatography. *Analyst* **2007,** *132,* 403-405.

(46) Peristyy, A. A.; Fedyanina, O. N.; Paull, B.; Nesterenko, P. N., Diamond Based Adsorbents and Their Application in Chromatography. *J. Chromatogr. A* **2014,** *1357,* 68-86.

(47) Chen, W.-H.; Lee, S.-C.; Sabu, S.; Fang, H.-C.; Chung, S.-C.; Han, C.-C.; Chang, H.-C., Solid-Phase Extraction and Elution on Diamond (Speed): A Fast and General Platform for Proteome Analysis with Mass Spectrometry. *Anal. Chem.* **2006,** *78,* 4228-4234.

(48) Peristyy, A.; Paull, B.; Nesterenko, P. N., Chromatographic Performance of Synthetic Polycrystalline Diamond as a Stationary Phase in Normal Phase High Performance Liquid Chromatography. *J. Chromatogr. A* **2015,** *1391,* 49-59.

(49) Korobov, M. V.; Avramenko, N. V.; Bogachev, A. G.; Rozhkova, N. N.; Ōsawa, E., Nanophase of Water in Nano-Diamond Gel. *J. Phys. Chem. C* **2007,** *111,* 7330-7334.

(50) Nesterenko, P. N.; Fedyanina, O. N., Properties of Microdispersed Sintered Nanodiamonds as a Stationary Phase for Normal-Phase High Performance Liquid Chromatography. *J. Chromatogr. A* **2010,** *1217,* 498-505.

(51) Wiest, L. A.; Jensen, D. S.; Hung, C. H.; Olsen, R. E.; Davis, R. C.; Vail, M. A.; Dadson, A. E.; Nesterenko, P. N.; Linford, M. R., Pellicular Particles with Spherical Carbon Cores and Porous Nanodiamond/Polymer Shells for Reversed-Phase Hplc. *Anal. Chem.* **2011,** *83,* 5488-5501.

(52) Fekete, S.; Jensen, D. S.; Zukowski, J.; Guillarme, D., Evaluation of a New Wide-Pore Superficially Porous Material with Carbon Core and Nanodiamond-Polymer Shell for the Separation of Proteins. *J. Chromatogr. A* **2015,** *1414,* 51-59.

(53) Liu, Y.; Khabashesku, V. N.; Halas, N. J., Fluorinated Nanodiamond as a Wet Chemistry Precursor for Diamond Coatings Covalently Bonded to Glass Surface. *J. Am. Chem. Soc.* **2005,** *127,* 3712-3713.

(54) Saini, G.; Jensen, D. S.; Wiest, L. A.; Vail, M. A.; Dadson, A.; Lee, M. L.; Shutthanandan, V.; Linford, M. R., Core−Shell Diamond as a Support for Solid-Phase Extraction and High-Performance Liquid Chromatography. *Anal. Chem.* **2010,** *82,* 4448-4456.

(55) Reynolds, K. J.; Colón, L. A., Submicron Sized Organo-Silica Spheres for Capillary Electrochromatography. *J. Liq. Chromatogr. Relat. Technol.* **2000,** *23,* 161-173.

(56) Cintron, J. M.; Colon, L. A., Organo-Silica Nano-Particles Used in Ultrahigh-Pressure Liquid Chromatography. *Analyst* **2002,** *127,* 701-704.

(57) Liang, Y.; Ozawa, M.; Krueger, A., A General Procedure to Functionalize Agglomerating Nanoparticles Demonstrated on Nanodiamond. *ACS Nano* **2009,** *3,* 2288-2296.

(58) Girard, H. A.; Petit, T.; Perruchas, S.; Gacoin, T.; Gesset, C.; Arnault, J. C.; Bergonzo, P., Surface Properties of Hydrogenated Nanodiamonds: A Chemical Investigation. *Phys Chem Chem Phys* **2011,** *13,* 11517-11523.

(59) Ando, T.; Ishii, M.; Kamo, M.; Sato, Y., Thermal Hydrogenation of Diamond Surfaces Studied by Diffuse Reflectance Fourier-Transform Infrared, Temperature-Programmed Desorption and Laser Raman Spectroscopy. *J. Chem. Soc., Faraday Trans.* **1993,** *89,* 1783-1789.

(60) Shenderova, O.; Panich, A. M.; Moseenkov, S.; Hens, S. C.; Kuznetsov, V.; Vieth, H. M., Hydroxylated Detonation Nanodiamond: Ftir, Xps, and Nmr Studies. *J. Phys. Chem. C* **2011,** *115,* 19005-19011.

(61) Wolcott, A.; Schiros, T.; Trusheim, M. E.; Chen, E. H.; Nordlund, D.; Diaz, R. E.; Gaathon, O.; Englund, D.; Owen, J. S., Surface Structure of Aerobically Oxidized Diamond Nanocrystals. *J. Phys. Chem. C* **2014,** *118,* 26695-26702.

(62) Larionova, I.; Kuznetsov, V.; Frolov, A.; Shenderova, O.; Moseenkov, S.; Mazov, I., Properties of Individual Fractions of Detonation Nanodiamond. *Diamond Relat. Mater.* **2006,** *15,* 1804-1808.

(63) Li, L.; Colon, L. A., Hydrosilylated Allyl-Silica Hybrid Monolithic Columns. *J. Sep. Sci.* **2009,** *32,* 2737-2746.

(64) Colon, H.; Zhang, X.; Murphy, J. K.; Rivera, J. G.; Colon, L. A., Allyl-Functionalized Hybrid Silica Monoliths. *Chem. Commun.* **2005**.

(65) Nichols, B. M.; Butler, J. E.; Russell, J. N.; Hamers, R. J., Photochemical Functionalization of Hydrogen-Terminated Diamond Surfaces: A Structural and Mechanistic Study. *J. Phys. Chem. B* **2005,** *109,* 20938-20947.

(66) Strother, T.; Knickerbocker, T.; Russell, J. N.; Butler, J. E.; Smith, L. M.; Hamers, R. J., Photochemical Functionalization of Diamond Films. *Langmuir* **2002,** *18,* 968-971.

(67) Wang, X.; Colavita, P. E.; Streifer, J. A.; Butler, J. E.; Hamers, R. J., Photochemical Grafting of Alkenes onto Carbon Surfaces: Identifying the Roles of Electrons and Holes. *J. Phys. Chem. C* **2010,** *114,* 4067-4074.

(68) Tsubota, T.; Mihara, S.; Murakami, N.; Ohno, T., Chemical Modification of Diamond Surface with Linoleic Acid by Using Benzoyl Peroxide. *Diamond Relat. Mater.* **2011,** *20,* 584-587.

(69) Tsubota, T.; Kawamura, Y.; Murakami, N.; Ohno, T., Chemical Modification of Diamond Surface with X–(C_6H_4)–COOH (X=F,Cl,Br, I) Using Benzoyl Peroxide. *Diamond Relat. Mater.* **2010,** *19,* 1003-1006.

(70) Dahoumane, S. A.; Nguyen, M. N.; Thorel, A.; Boudou, J.-P.; Chehimi, M. M.; Mangeney, C., Protein-Functionalized Hairy Diamond Nanoparticles. *Langmuir* **2009,** *25,* 9633-9638.

(71) Jarre, G.; Liang, Y.; Betz, P.; Lang, D.; Krueger, A., Playing the Surface Game-Diels-Alder Reactions on Diamond Nanoparticles. *Chem. Commun.* **2011,** *47,* 544-546.

Table of Content

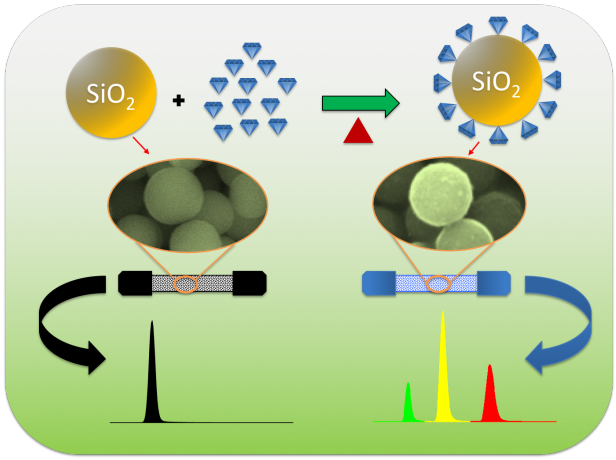

Supporting Information

Nanodiamond-decorated silica spheres as a chromatographic material

*Zuqin Xue, John C. Vinci, Luis A. Colón**

Department of Chemistry, Natural Sciences Complex,

University at Buffalo, The State University of New York

Buffalo, New York 14260-3000, United States

*Corresponding author: lacolon@buffalo.edu

Scheme S1. Simplified schematic representation of the reactions of hydrogenated nanodiamonds (ND) with allyl-silica particles using benzoyl peroxide (BPO) as a radical initiator**.**

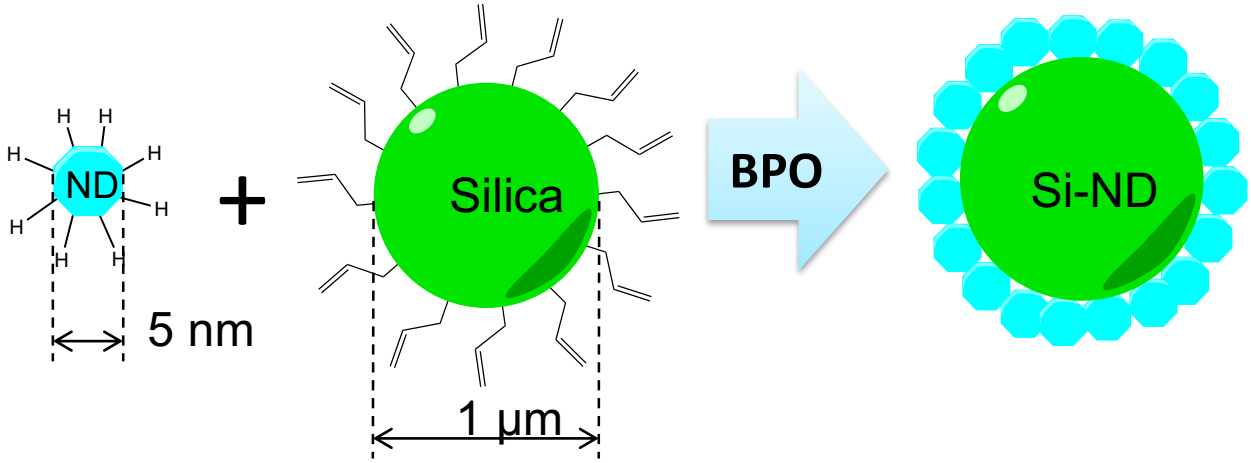

$(C_6H_5–COO)_2 \xrightarrow{heat} 2\ C_6H_5–COO•$ (BzO•= $C_6H_5–COO•$)

BzO• + H–(ND) ----> BzOH + •(ND)

BzO• + (organo–Silica) ----> BzOH + •(organo–Silica) [or •(BzO–organo–Silica)]

(organo–Silica)• + •(ND) ----> ND–(organo-Silica)

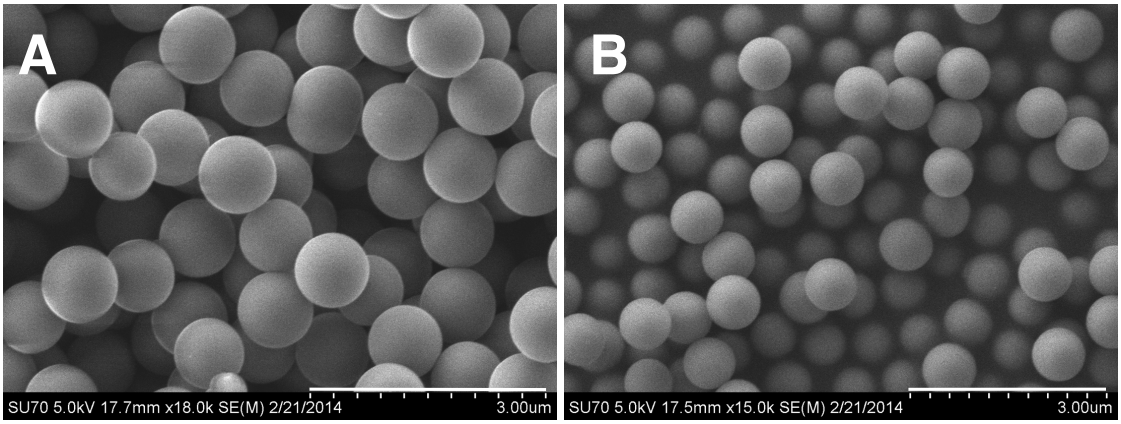

Figure S1. SEM images of A) bare silica particles and B) allyl-silica particles (note that the image in A is of a slightly higher magnification).

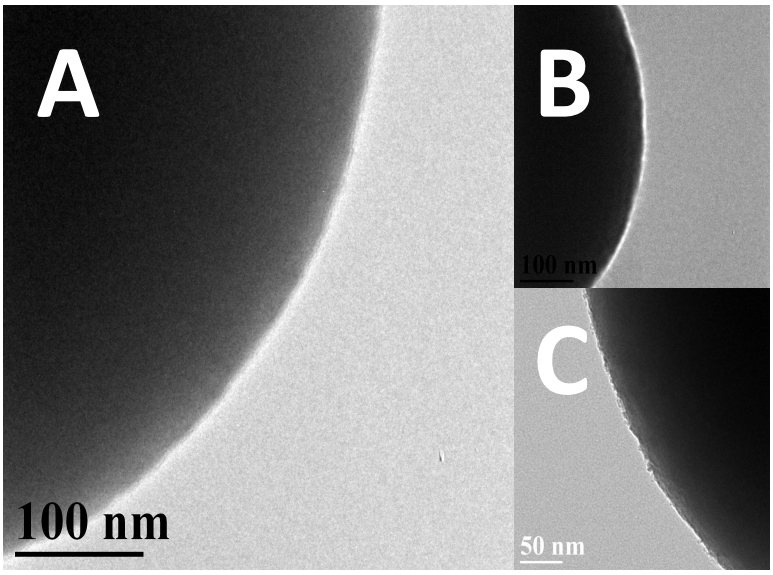

Figure S2. TEM images of A) allyl-silica, B) allyl-silica exposed to O-NDs and C) allyl-silica exposed to H_2-NDs; in all cases without UV light (i.e., in the dark). ND adsorption was not observed.

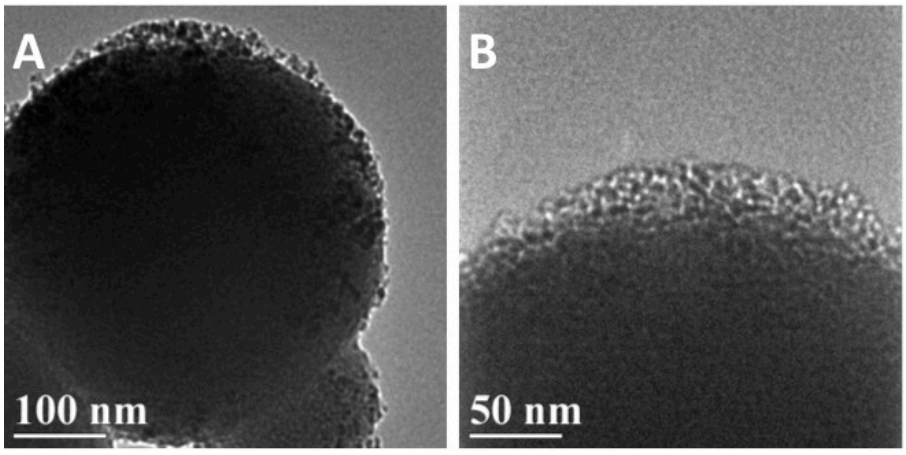

Figure S3. TEM images of allyl-silica modified with H_2-NDs using BPO as the reaction initiator at different magnifications: A) 100 nm B) 50 nm.

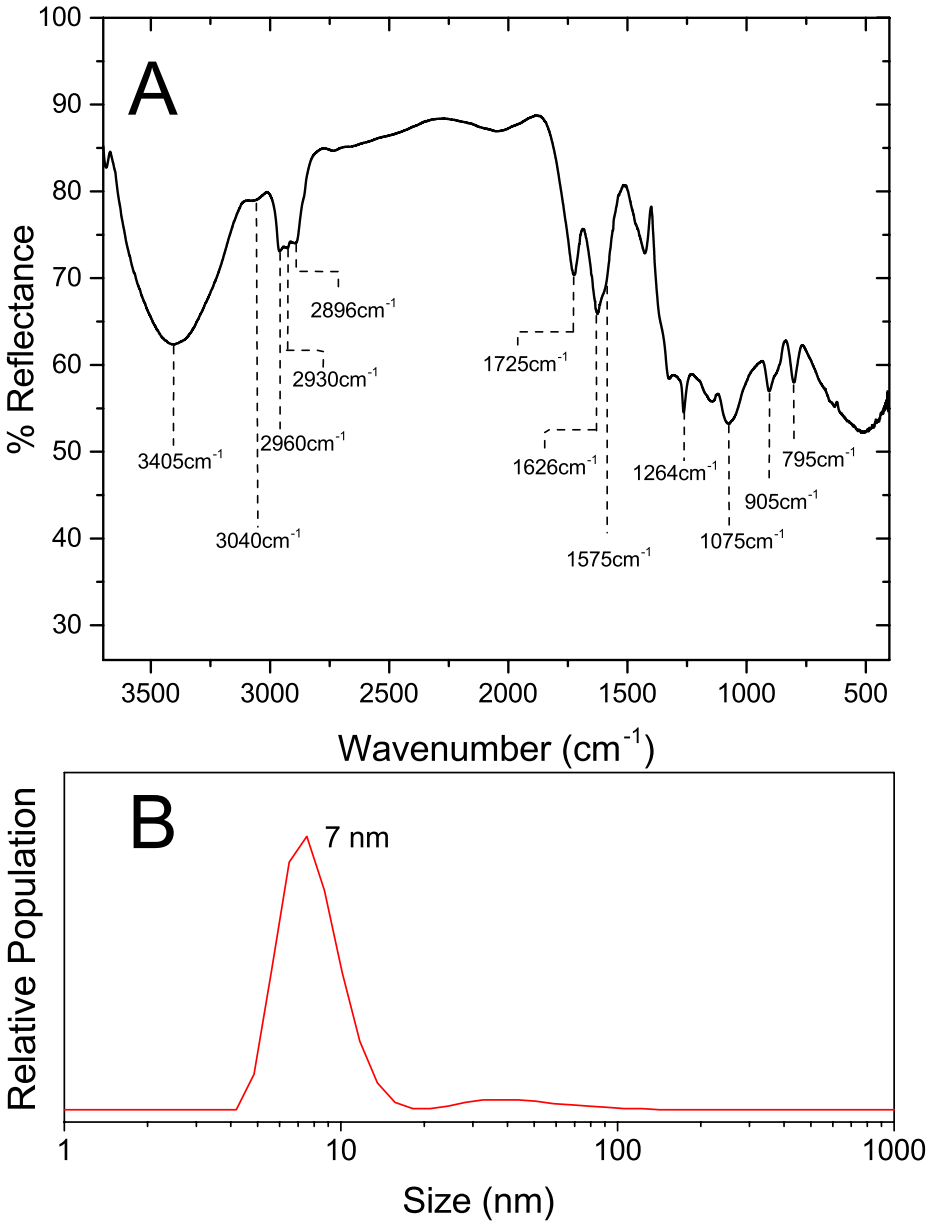

Figure S4. (A) DRIFT spectrum of C-NDs. For peak assignment to a respective functional group see Table S5. (B) Particle size distribution of C-NDs.

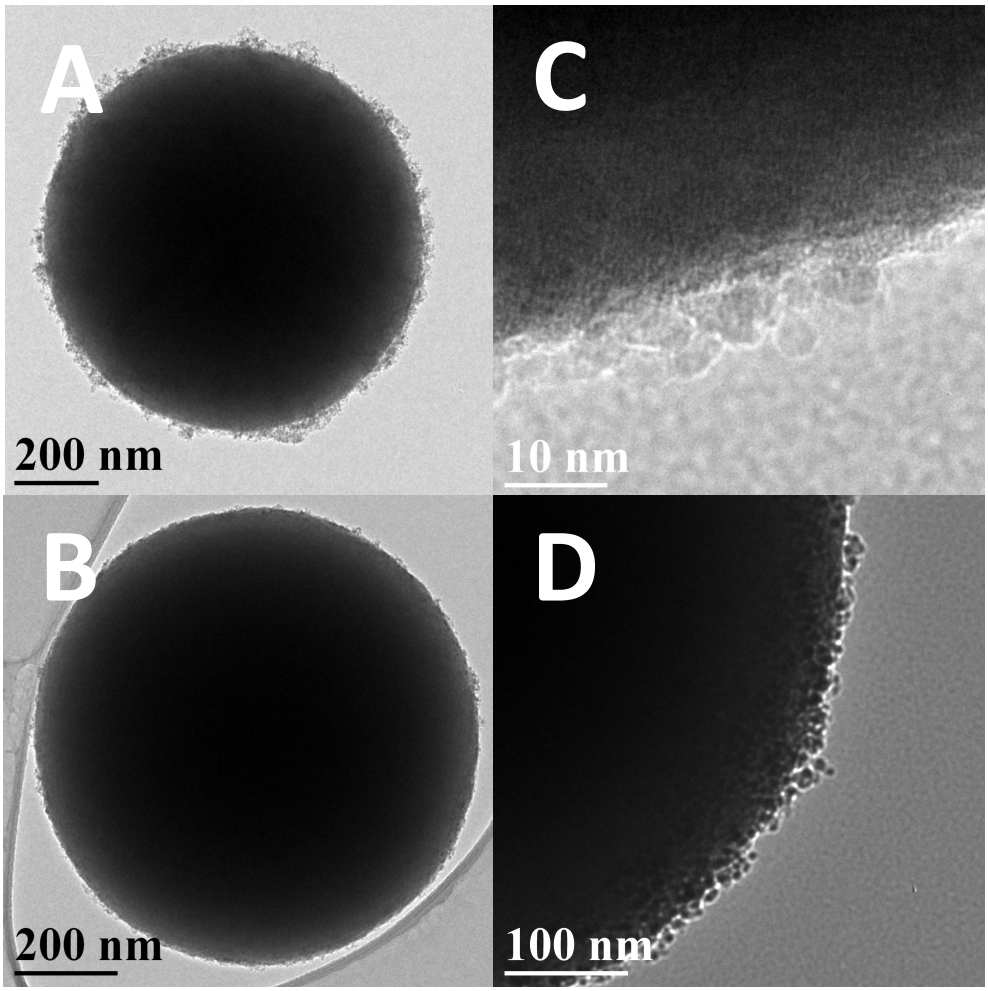

Figure S5. TEM of C-NDs on silica particles produced by BPO-initiated reaction of C-NDs and allyl-silica prepared by A) microwave heating (75 °C), B) reaction under horn sonication programmed maintain to a temperature of 80 °C, C) higher magnification of B), and D) prepared by heating at 90 °C in an oil bath. The TEM images suggest that one could control the thickness of the ND layer by manipulating the processing parameters. For example, Figure 5SB shows a thickness of about 5-10 nm when coupling using heating (80°C) and horn sonication during the reaction. However, when microwave heating (75°C) without horn sonication was used, a thicker (albeit irregular thickness) layer of ND was produced (20-50nm). Further, by heating the reaction at 90°C in an oil bath along produced a thickness of about 30 nm.

Table S1. Peaks and corresponding vibration assignments for spectrum in Figure 2A (H_2-NDs).[1-8]

Wavenumber (cm^{-1})	Vibration
3600-3200	O-H
2943	C-H
2878	C-H
1697	C=O
1664	C-H
1630	O-H
1571	C-C
1260	C-O-C
1081	C-O-C
918	C-H
795	C-H

Table S2. Peaks and corresponding vibration assignments for spectrum in Figure 2B (O-NDs).[1-3,7-9]

Wavenumber (cm^{-1})	Vibration
3600-3200	O-H
3038	C-H
2964	C-H
2910	C-H
2845	C-H
1750	C=O
1620	O-H
1225	C-O-C
1058	C-O-C
855	C-O
589	C-O

Table S3. Relative elemental surface composition by XPS for bare-silica, allyl-silica, H_2-ND allyl-silica, and OD-ND allyl-silica (UV-initiated reactions).

Sample	C	O	Si
Bare-silica	4	68	28
Allyl-silica	22	54	24
Allyl-silica + H_2-ND (UV)	49	37	14
Allyl-silica + O-ND (UV)	49	40	12
Allyl-silica + O-ND (dark)	24	55	21

Table S4. Peaks and corresponding vibration assignments for spectrum in Figure 4 (silica and ND-modified silica particles).[10-13]

Wavenumber (cm^{-1})	Vibration
3081	=C-H
2978	C-H
2934	C-H
1690	C=O
1635	C=C, O-H
1630	O-H
1466	C-H
1421	C-H

Table S5. Peaks and corresponding vibration assignments for spectrum in Figure S4 (C-NDs).[1-3,7,8]

Wavenumber (cm^{-1})	Vibration
3686	isolated O-H
3405	O-H
3040	C-H
2960	C-H
2930	C-H
2896	C-H
1725	C=O
1626	O-H
1575	C-C
1264	C-O-C
1075	C-O-C
905	C-H
801	C-H

REFERENCES

(1) Huang, L. C. L.; Chang, H.-C. Adsorption and Immobilization of Cytochrome C on Nanodiamonds. *Langmuir* **2004,** *20,* 5879-5884.

(2) Shenderova, O.; Panich, A. M.; Moseenkov, S.; Hens, S. C.; Kuznetsov, V.; Vieth, H. M. Hydroxylated Detonation Nanodiamond: FTIR, XPS, and NMR Studies. *J. Phys. Chem. C* **2011,** *115,* 19005-19011.

(3) Tu, J.-S.; Perevedentseva, E.; Chung, P.-H.; Cheng, C.-L. Size-Dependent Surface CO Stretching Frequency Investigations on Nanodiamond Particles. *J. Chem. Phys.* **2006,** *125,* 174713.

(4) Ando, T.; Ishii, M.; Kamo, M.; Sato, Y. Thermal Hydrogenation of Diamond Surfaces Studied by Diffuse Reflectance Fourier-Transform Infrared, Temperature-Programmed Desorption and Laser Raman Spectroscopy. *J. Chem. Soc., Faraday Trans.* **1993,** *89,* 1783-1789.

(5) Ando, T.; Inoue, S.; Ishii, M.; Kamo, M.; Sato, Y.; Yamada, O.; Nakano, T. Fourier-Transform Infrared Photoacoustic Studies of Hydrogenated Diamond Surfaces. *J. Chem. Soc., Faraday Trans.* **1993,** *89,* 749-751.

(6) Ando, T.; Ishii, M.; Kamo, M.; Sato, Y. Diffuse Reflectance Infrared Fourier-Transform Study of the Plasma Hydrogenation of Diamond Surfaces. *J. Chem. Soc., Faraday Trans.* **1993,** *89,* 1383-1386.

(7) Osipov, V. Y.; Aleksenskiy, A. E.; Shames, A. I.; Panich, A. M.; Shestakov, M. S.; Vul', A. Y. Infrared Absorption Study of Surface Functional Groups Providing Chemical Modification of Nanodiamonds by Divalent Copper Ion Complexes. *Diamond Relat. Mater.* **2011,** *20,* 1234-1238.

(8) Larionova, I.; Kuznetsov, V.; Frolov, A.; Shenderova, O.; Moseenkov, S.; Mazov, I. Properties of Individual Fractions of Detonation Nanodiamond. *Diamond Relat. Mater.* **2006,** *15,* 1804-1808.

(9) Stehlik, S.; Varga, M.; Ledinsky, M.; Jirasek, V.; Artemenko, A.; Kozak, H.; Ondic, L.; Skakalova, V.; Argentero, G.; Pennycook, T.; Meyer, J. C.; Fejfar, A.; Kromka, A.; Rezek, B. Size and Purity Control of HPHT Nanodiamonds Down to 1 nm. *J. Phys. Chem. C* **2015**, *119*, 27708-27720.

(10) Colón, H.; Zhang, X.; Murphy, J. K.; Rivera, J. G.; Colón, L. A. Allyl-Functionalized Hybrid Silica Monoliths. *Chem. Commun.* **2005,** *22*, 2826-2828.

(11) Reynolds, K. J.; Colón, L. A. Submicron Sized Organo-Silica Spheres for Capillary Electrochromatography. *J. Liq. Chromatogr. Relat. Technol.* **2000,** *23,* 161-173.

(12) Misran, H.; Yarmo, M. A.; Ramesh, S. Synthesis and Characterization of Silica Nanospheres Using Nonsurfactant Template. *Ceram. Int.* **2013,** *39,* 931-940.

(13) Sankaraiah, S.; Lee, J. M.; Kim, J. H.; Choi, S. W. Preparation and Characterization of Surface-Functionalized Polysilsesquioxane Hard Spheres in Aqueous Medium. *Macromolecules* **2008,** *41,* 6195-6204.